Robotica (2016) volume 34, pp. 1090–1112. © Cambridge University Press 2014
doi:10.1017/S0263574714002082

A novel movement-based operation method for dual-arm rescue construction machinery

Cheng Fang* and Xilun Ding

Robotics Institute, Department of Mechanical Engineering and Automation, Beihang University, Beijing City, 100191, P. R. China

(Accepted July 2, 2014. First published online: August 11, 2014)

SUMMARY

The issue of the operation method for dual-arm rescue construction machinery is investigated in this paper. To increase its operational efficiency and to save more time at rescue sites, some operating strategies of the human arm are employed to design a novel operation method for construction machinery. On the basis of that, a novel and anthropomorphic task-motion planning and performing framework for rescue construction machinery is established. Firstly, the main tasks construction machinery encounter are summarized, and then, these tasks are decomposed to several manipulation and movement sequences. Finally, several frequently used movements, which consist of some basic movement elements, are designed to be intuitive movement primitives coordinating related movement elements simultaneously to improve the operational efficiency, which forms a novel operation method for rescue construction machinery. Additionally, in order to avoid the potential collision between the dual arms, a self-collision avoidance surveillance method is proposed to guarantee the safety of the novel operation method. An application case is presented to introduce the proposed method specifically, and a typical simulation of a dual-arm grip-and-cut task is carried out to verify the feasibility and effectiveness of the framework.

KEYWORDS: Rescue construction machinery; Operation method; Movement library.

1. Introduction

At present, people's lives and property are continually jeopardized by many kinds of disasters, such as earthquakes, debris flows, fire disasters, explosions, terrorist activities, and major accidents in production. In recent years, China has a high incidence of earthquakes, for example, the 5.12 Wenchuan earthquake and the 4.14 Yushu earthquake that shocked the world. Hence, the study on rescue construction machinery has gained wide attention, and some research progress has been made, which is mainly involved with some intelligent techniques for small-scale construction machinery or robots such as detection, sensation and so on, but it seems we paid little attention on the research about the manipulation ability of large-scale rescue construction machinery in intricate ruins.

However, the large heavy mechanized equipment is often required in the rescue tasks which rescue crew can not achieve manually or achieve in very low efficiency. So, in order to overcome these difficulties, we try to research and develop a kind of large rescue mechanized equipment which has the capacity to handle the remains of buildings rapidly and accurately to meet the demand. There are various tasks in the rescue sites, typically including cutting, smashing, segmenting the remains of buildings, cleaning, grasping, and transferring the debris. The approach employed widely to meet various task demands mentioned above is to switch different tools at the extremity of the manipulator of construction machinery. Typical tools include the grab, the hydraulic shear, the breaking hammer, the drilling tool, and the expander. It is well-known that time is life in the rescue process, and rescue efficiency is very crucial for the rescue work. However, switching tools frequently will sacrifice operational efficiency undoubtedly. In addition, some work can not be accomplished by single manipulator such as hauling something under a flat collapsed wall, grasping a large object and

* Corresponding author. E-mail: fcdean@163.com

https://doi.org/10.1017/S0263574714002082 Published online by Cambridge University Press

cutting it, bending a long object, etc. So, we try to introduce dual-arm configuration to improve the manipulation capacity and the efficiency of construction machinery. Specifically, two standard tools are installed at the extremities of the dual arms respectively to deal with the majority of tasks in a coordinated manner. At the same time, tools can be exchanged from a tool holder to adapt to other tasks if necessary.

From the robotic point of view, the dual-arm coordinated manipulation is an important way to resolve the problem on complicated tasks in the extreme environment. The typical examples of the dual-arm robots are Robonaut (developed by NASA) and Rollin Justin (developed by DLR) which both have anthropomorphic upper body and dual-arm structure, and both be expected to help human astronauts achieve dangerous work in outer space environment.[1,2] Disaster relief is also an area with extreme environment, and is a main application area of special robots. For this reason, applying some planning approaches and control policies in robotics to rescue construction machinery is an inevitable development trend. Recently, more and more construction machines become intelligent, and their appearance are more like robots,[3,4] which is a proof of the trend. However, it is worth noting that there are also a lot of important distinctions between the dual-arm systems employed in the robotic field and the construction machinery field. In the robotic area, the majority of practical applications for dual-arm systems can be mainly and roughly divided into industrial applications and domestic applications.[5] The typical industrial applications of the dual arms are parts assembly[6] and material reshaping,[7] while the typical domestic applications include folding laundry[8] and attendant care for the elderly.[9] Since the dual arms are often required to manipulate the same object or a pair of objects being connected to form a closed chain in industrial applications, the issue of how to employ a proper control law to coordinate such a system is mainly discussed.[10] And in the domestic applications, because of the indispensable physical interaction between dual-arm systems and human beings, the control policies used to direct dual-arm systems interact with people need to be taken into account.[11] In addition, according to the definition and classification of dual-arm manipulation in the literature,[5] most of tasks faced by dual-arm systems in the robotic field belong to the bimanual manipulation which is defined as physically interacting with the same object and is one type of dual-arm manipulation. However, the majority of the manipulation tasks faced by rescue construction machinery belong to the other type of dual-arm manipulation, goal-coordinated manipulation, in which dual arms perform different parts of the same task almost without interacting with one another. So, the major problem we should consider in this case is how to increase the efficiency of the coordinated manipulation as much as possible.

Therefore, from the perspective of biologically-inspired robots, one of our major contributions to the goal-coordinated dual-arm manipulation is to apply the idea of movement primitive, one important strategy of the human dual-arm manipulation, to the construction machinery field to form an intuitive and intelligible operation method for operators, which provides a novel method for the operation of construction machinery. Schaal, S.[12] also proposed the concept of movement primitive to make robots simulate some rhythmic movements observed in some tasks people perform. In the paper, the nonlinear dynamical systems are employed to realize the movement primitives for the single joint. Two basic movement primitive types, point-to-point movement primitive created by the discrete dynamic system and oscillatory movement primitive generated by the rhythmic system, are used to be combined into desired motion for the single joint. And a phase-offset coordination technique is employed to generate multi-joint rhythmic movement for anthropomorphic arms or even humanoid robots. However, according to the result of an investigation report,[13] the task types rescue construction machinery face during the phase of debris excavation at the disaster sites are limited and seemingly don't belong to the typical rhythmic movements. In addition, an additional coordinated mechanism is designed in this paper to implement multi-joint complex movements, while our proposed primitives are directly in the form of multi-joint coordinated motion. So, these two kinds of movement primitives are different. Furthermore, our proposed primitives applied in the operation of rescue construction machinery also differ from primitives people always employ. As four, T.[14] explored the method to realize the skill transfer from the human body to the robot. First, according to some designed indices in the joint space and operational space, several "key points" are extracted from the demonstrated movements to be used to train corresponding HMMs. By comparing the HMM state sequences and selecting only those states that appear in every sequence, some "common key points" are found to be employed to guide the reproduction of the movement on the robot. However, the structure of the dual arms of rescue construction machinery is very different from the structure of the human dual arms.

https://doi.org/10.1017/S0263574714002082 Published online by Cambridge University Press

So, our research does not refer to the exact imitation of the human dual-arm movement. We just try to make the dual arms of rescue construction machinery simulate the same movement primitives as we could do in a certain operational task in terms of operational space or task space, but not the whole configuration space. In this way, on one hand, the operator can operate the construction machine in the way he uses his own dual arms to achieve complicated tasks, so that his operation effort can be effectively alleviated. On the other hand, one movement primitive, as several coordinated motions of its multiple internal joints, can be carried out by only one operational action. Compared with the traditional method of operating a single joint at each operational action, the proposed operation method can greatly improve the operational efficiency.

In addition, because both the dual-arm robots and dual-arm construction machines are prone to collision between their dual arms, a self-collision avoidance surveillance method between dual arms is proposed in this paper to monitor the running state of the dual arms, which is our another major contribution to the dual-arm manipulation. For collision detection, in order to simplify the process and reduce the computation cost, geometric objects (different links of the dual arms in this case) are enclosed inside simple bounding volumes such as Cylinders,[15,16] Axis Aligned Bounding Box (ABB),[17] Oriented Bounding Box (OBB),[18] etc. However, these bounding volumes usually including the larger safety margin around each link will significantly decrease the range of movement of a joint. So, in order to obtain enough range of movement and safety margin, Kei Okada[19] developed hybrid approach that uses both table based collision checking for compound joints and online geometrical model checking with a simplified link shape for other joints. Because the two factors, operational efficiency and safety, are emphasized greatly during the rescue process. We ignore the reduction of the joint range of motion and propose to employ another kind of bounding volume, Sphere-Swept Volume (SSV), to approximately represent the shapes of the links in order to realize rapid collision detection between the dual arms in the rescue field. According to the knowledge of Computer Graphics, the computation of the minimum distance between two SSVs is quite simple, so, the SSV is recommended as an ideal bounding volume.

2. Task-Motion Planning and Control Framework of Anthropomorphic Dual-Arm Robots based on Movement Library

When people use their dual arms to achieve a specific task, the task will firstly be decomposed into two manipulation sequences for the left arm and the right arm by their experience. The manipulation sequence for each arm contains a series of major manipulation steps in proper order, which is a strategic-level planning, and each manipulation step can be further divided into several relatively independent movements that constitute a movement sequence, that is, a manipulation step corresponds to a movement sequence. A movement is defined as one move of the anthropomorphic arm that has an explicit and intuitive meaning. It is well-known that one human arm has a 3-DOF shoulder joint, a 2-DOF elbow joint, and a 2-DOF wrist joint. The individual motion caused by one DOF is regarded as movement element here. Obviously, all the motions of the human arm are composed of these seven movement elements. In recent years, more and more study results from neurophysiology manifest that the whole motion of the human arm is composed of several movement primitives.[20–24] These study results show that human arms can record some experience and motion modes after continually performing abundant daily tasks. Some movement elements gradually begin to form independent movement modules that are caused by several DOFs in a coordinated manner.[25–28] These are movement primitives, such as raising the hand, waving the hand, pushing, and so on. If one would like to run a movement primitive, he just needs to start a corresponding motion mode. In this way, people combining several movement primitives to realize a complex motion are just like building blocks, and people do not need to consider how every DOF moves so that the cognitive burden of the operator can be alleviated.[29] So this strategy of the human dual arms is applied to our task-motion planning framework of anthropomorphic dual-arm robots. Seven fundamental movement elements and several movement primitives can be regarded as the movement library of an anthropomorphic dual-arm robot, and several reasonable movements from the library constitute a movement sequence, that is, a manipulation step, and several manipulation steps further constitute a manipulation sequence, and two manipulation sequences of the dual arms finally realize the specific task. The whole task-motion planning framework is shown in Fig. 1.

https://doi.org/10.1017/S0263574714002082 Published online by Cambridge University Press

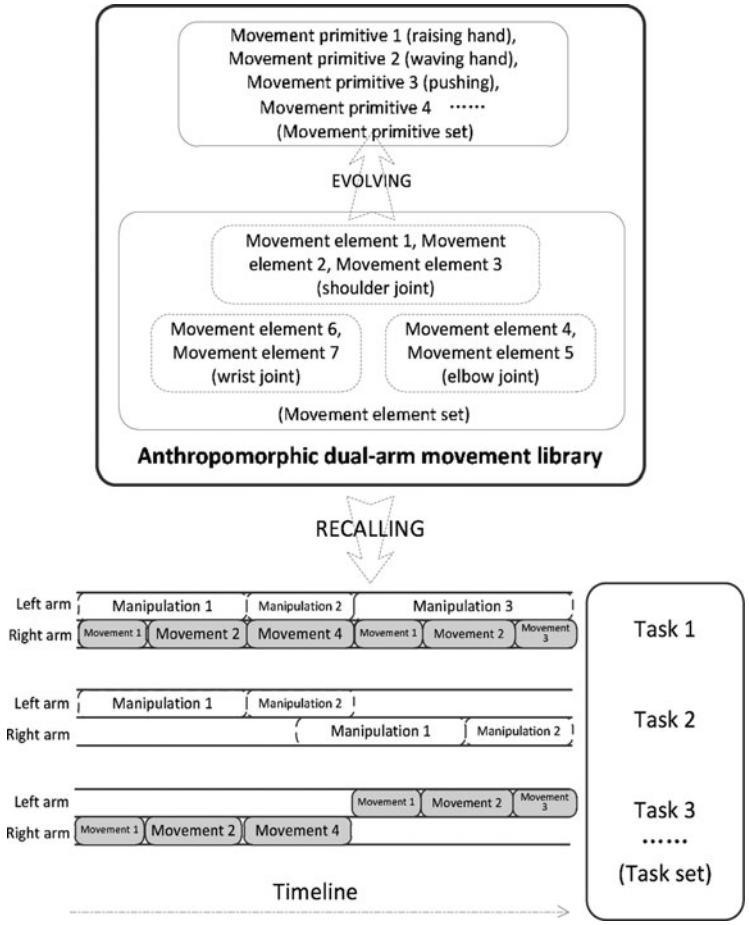


Fig. 1. Task-motion planning framework of anthropomor-phic dual-arm robots.

3. Application of the Task-Motion Planning of Anthropomorphic Dual-Arm Robots to Rescue Construction Machinery

For rescue construction machinery, the most important requirement is operational efficiency, which has an important influence on the rescue time and rescue effect. A movement primitive, as a coordinated and simultaneous motion of several movement elements, can be referred to as a very desirable manner to save time during the operation, since the operator does not need to carry out every movement element in turn. In this section, we will apply the proposed task-motion planning framework for the anthropomorphic dual-arm robots to rescue construction machinery. The first question is how to design or extract the reasonable movement primitives. It is worth noting that the extraction of the movement primitives mainly depends on the specific application field. Hence, we should first get familiar with the operation tasks that rescue construction machinery may face. We will decompose each task into several bigger manipulation steps and further into smaller movements at the level of task space, which is in accordance with our operation habit. And then, the results of the decompositions for these tasks are summarized, and several frequently used movement modules caused by coordinated motions of multiple joints are designed as reusable movement primitives. Because the strategy of the task decomposition and the designed primitives are easy for the operators to understand, the use of the primitive will reduce the operation effort of the operators and increase their operational efficiency. According to the rescue scene, there are, for the most part, five types of tasks for rescue construction machinery: grasp the remains of buildings and debris, and then transfer them to load, cut reinforced concrete and cables, demolish and smash large buildings, drill holes through hard walls, and hold up large heavy objects. The rescue construction machine accomplishes these five types of tasks by installing different tools at the extremity of its manipulators. Table I lists five tools corresponding to the five tasks mentioned above, and Fig. 2 is a real picture for them.

https://doi.org/10.1017/S0263574714002082 Published online by Cambridge University Press

Table I. Five main tasks of rescue construction machinery and corresponding tools.

	Main tasks	Main tools
1	Grasping, transferring and loading	Grab
2	cutting	Hydraulic shear
3	Demolishing and smashing	Breaking hammer
4	Drilling	Drilling tool
5	Supporting	Expander

Table II. Manipulation and movement sequences of grasping and transferring task.

Manipulation sequence	Movement sequence	Grasping and transferring task
1 Preparation manipulation	1	Move the grab to approach the target.
	2	Adjust the orientation of the grab.
	3	Finely adjust the posture of the grab.
2 Executing manipulation	4	Close the grab.
3 Transferring manipulation	5	Transfer the grab to the specified location.
	6	Adjust the orientation of the grab.
4 Executing manipulation	7	Open the grab.

Table III. Manipulation and movement sequences of cutting task.

Manipulation sequence	Movement sequence	Cutting task
1 Preparation manipulation	1	Move the hydraulic shear to approach the target.
	2	Adjust the orientation of the hydraulic shear.
	3	Finely adjust the posture of the hydraulic shear.
2 Executing manipulation	4	Movement of the hydraulic shear.

Table IV. Manipulation and movement sequences of demolishing and smashing task.

Manipulation sequence	Movement sequence	Demolishing and smashing task
1 Preparation manipulation	1	Move the breaking hammer to approach the target.
	2	Adjust the orientation of the breaking hammer.
	3	Finely adjust the posture of the breaking hammer.
2 Executing manipulation	4	Feed movement of the breaking hammer along its orientation.



Fig. 2. Real pictures of the five tools.

Tables II–VI describe the manipulation and movement sequences respectively, when the rescue construction machine individually installs the five tools mentioned above to achieve corresponding tasks.

It is not difficult to find that the movements of the five different tasks are almost the same in the preparation and manipulation stage, in which finely adjusting the posture of the tool denotes the movement combination of further accurately moving the position of the tool and adjusting its

https://doi.org/10.1017/S0263574714002082 Published online by Cambridge University Press

Table V. Manipulation and movement sequences of drilling task.

Manipulation sequence	Movement sequence	Drilling task
1 Preparation manipulation	1	Move the drilling tool to approach the target.
	2	Adjust the orientation of the drilling tool.
	3	Finely adjust the posture of the drilling tool.
2 Executing manipulation	4	Feed movement of the drilling tool along its orientation and the self-rotation movement.

Table VI. Manipulation and movement sequences of supporting task.

Manipulation sequence	Movement sequence	Supporting task
1 Preparation manipulation	1	Move the expander to approach the target.
	2	Adjust the orientation of the expander.
	3	Finely adjust the posture of the expander.
2 Executing manipulation	4	Feed movement of the expander along its orientation.
	5	Movement of the expander.

orientation. In the traditional joint operational mode of rescue construction machinery, the movement of moving the tool is realized by adjusting the movement elements of the main and auxiliary arms in turn, while the movement of adjusting the orientation of the tool is achieved by moving the joints in the wrist in turn. So for convenience, we can design an independent movement primitive for the movement of moving the tool in order to directly and intuitively control the center of the wrist of the tool by simultaneously coordinating the motions of different movement elements. Because of the limited range of motion and intrinsic intuitiveness, we did not design an independent movement primitive for the movement of adjusting the orientation of the tool. We also notice that there is always a feed movement of the tool along its orientation in the smashing, drilling and supporting tasks. Since this kind of movements is used frequently and is also a motion coordination of many movement elements, we design a movement primitive for it to facilitate the operation. The operation effect of the primitive is to move the tool forward and backward along its orientation. Based on the discussion above, we get two movement primitives for rescue construction machinery: moving the tools and feeding the tool along its orientation. Then, the two movement primitives and the basic movement elements constitute a movement library together for rescue construction machinery. For rescue construction machinery, a kind of automation equipment containing many DOFs, the movement primitives in the movement library can alleviate the operational burden of operators to help them operate the dual arms of the machine more intuitively and conveniently.

4. A Case Study of the Task-Motion Planning and Control for a Specific Dual-Arm Rescue Construction Machine

At present, almost all of the existing dual-arm rescue construction machines are from Japan. Tmsuk developed a series of products–T5, T52, and T53 in 2000, 2004, and 2007 respectively, and a dual-arm rescue construction machine, ASTACO, is produced by Hitachi Construction Machinery in 2011. But these construction machines are too light (T53 weighs 2.9 t, and ASTACO weighs 13.4 t), can only deal with small light objects, and can hardly satisfy the needs in disaster scene. Our project is to develop a series of disaster-relief-oriented intelligent dual-arm rescue construction machine products. Specifically, we will provide three kinds of products—large (60 t), medium (40 t), and small (20 t), that can be operated in the cab or be remotely controlled through wireless video transmission and can move by wheel or track. The maximum grasping weight of a single arm for them is 4 t, 8 t, and 10 t, respectively. In addition, they have many tools that can be rapidly exchanged to adapt to different tasks. Now, the 20 t product is under development; the three-dimensional simulation model of its prototype is shown in Fig. 3.

In Fig. 3, dual arms have the same structures that both consist of the main arm, the auxiliary arm, the wrist, and the tool; and they both have six DOFs (not including the DOF of the tool movement), which are the main arm swing, the main arm luffing, the auxiliary arm luffing, the tool luffing, the

https://doi.org/10.1017/S0263574714002082 Published online by Cambridge University Press

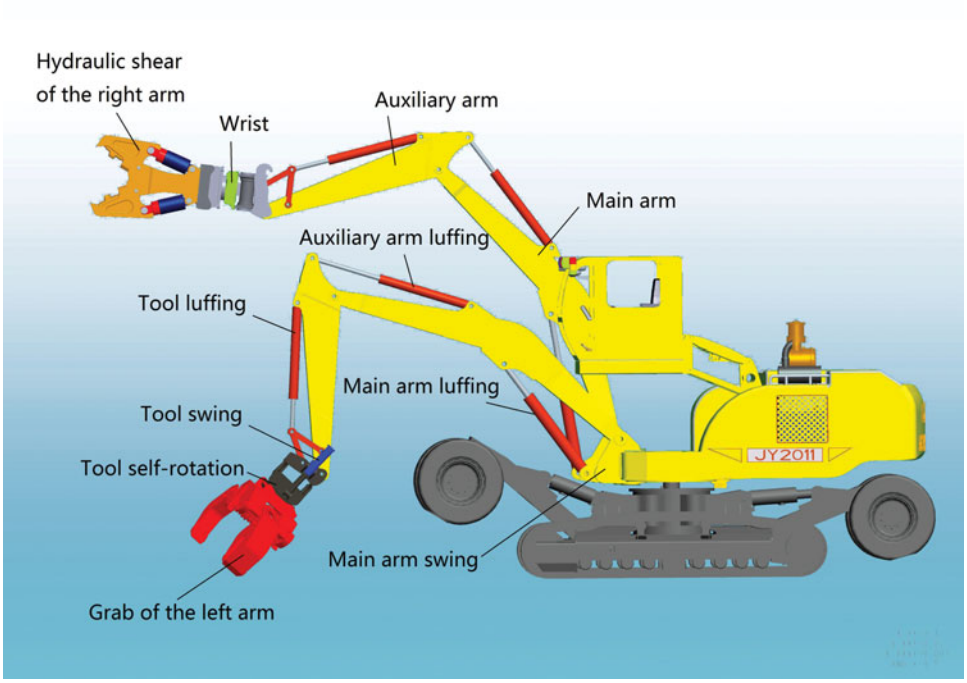


Fig. 3. Simulation model of the 20t prototype.

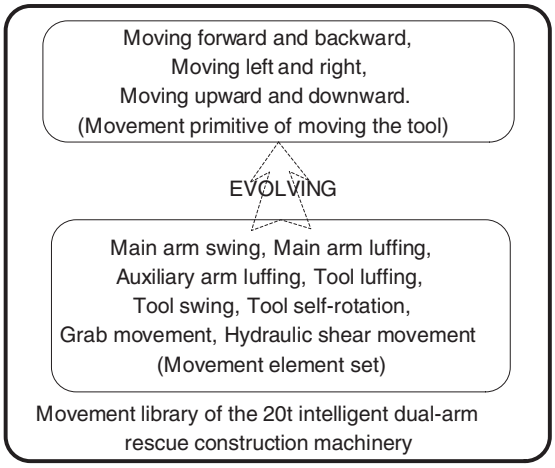


Fig. 4. Movement library of the 20t product.

tool swing, and the tool self-rotation from the cab to the extremity of the arm. According to the frequency of use of the tools, we use the typical configuration that employs the grab for the left arm and the hydraulic shear for the right arm. Because of nonexistence of the feed movement for the two tools, we only retain the movement primitive of moving the tool for the 20t product. In this case, this primitive is realized by coordinated motions of the main arm swing, main arm luffing, and auxiliary luffing; and its target is to control the position of the articulated point between the auxiliary arm and the wrist. Furthermore, it can be subdivided into three standard movement sub-primitives: moving the tool forward and backward, moving it leftward and rightward, and moving it upward and downward. The movement primitive of moving the tool can be one of the three sub-primitives or the combination of them. Hence, the specific movement library of the 20t product is shown in Fig. 4.

https://doi.org/10.1017/S0263574714002082 Published online by Cambridge University Press

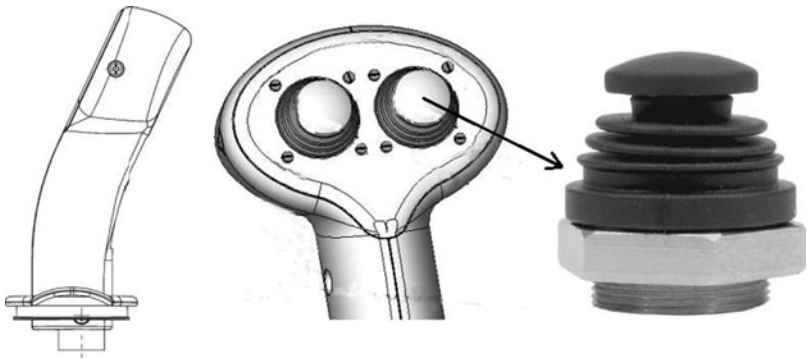


Fig. 5. Picture of the operating lever.

5. Several Specific Issues in the Design of the Dual-Arm Coordinated Operation

5.1. Human-machine interface design of the dual-arm coordinated operation

The movement primitive of moving the tool is actually an operational mode for construction machinery that can be called tool position operational mode. The position of the tool (actually the articulated point between the auxiliary arm and the tool) is controlled by the coordinated motions of the main arm swing, the main arm luffing, and the auxiliary arm luffing, which are automatically computed by a built-in algorithm introduced in section 5.2. This operational mode and the traditional joint operational mode, which controls a single movement element each time, constitute the operation method for the 20 t dual-arm rescue construction machine product. These modes are realized by two operating levers for the left and the right hands of the operator. The picture of a single operating lever is shown in Fig. 5.

Left and right operating levers are used to control the movements of the left arm and the right arm respectively. There are two small operating levers on the panel of each main operating lever, which can be moved forward, backward, leftward, and rightward like the main lever. So there are seven actions for each operating lever in all, including a rotation action of the main operating lever. In order to avoid misoperation, we enable the movement to execute by selecting the corresponding button on the control panel. In addition, the switch of different operational modes is realized by the correlated button on the control panel. The meaning of every action of the operating lever in these two operational modes is expressed in Figs. 6 and 7, respectively.

It is worth noting that these adverbs–forward, backward, left, right, upward, and downward–are described in terms of the operator in the cab. We put the operational actions of the adjacent movement elements as close as possible to facilitate the use of the operating lever. We also reduce the changes of the meaning of the operating levers when switching two operational modes as far as possible in order to alleviate the thinking burden of the operator. Based on this principle, we just change the meaning of the three actions of the main operating lever between two modes. Based on the lever action design, the operator can still adjust the orientation of the tool by the same actions of two small operating levers in tool position operational mode after moving the tool to the ideal position by the main operating lever. In addition, several movements can be carried out simultaneously when corresponding enabling action buttons on the control panel are selected. For example, pushing the main operating lever rightward and forward in the tool position operational mode can make the tool move rightward and forward.

5.2. Implementation of the movement primitive of moving the tool

The movement primitive of moving the tool is implemented by the coordinated motions of the main arm swing, the main arm luffing, and the auxiliary arm luffing. So how are the motions of these three movement elements controlled to cause the tool to move in the desired direction and velocity? The specific implementation algorithm is introduced in the following part. The single arm of the 20 t product is modeled by adopting the D-H method in robotics.[30]

Fig. 8 can be regarded as the right view of the simplified diagram of the arm of the 20 t product, where the vertical dashed line that passes through points O_0 and O_1 is the rotation axis of the main

https://doi.org/10.1017/S0263574714002082 Published online by Cambridge University Press

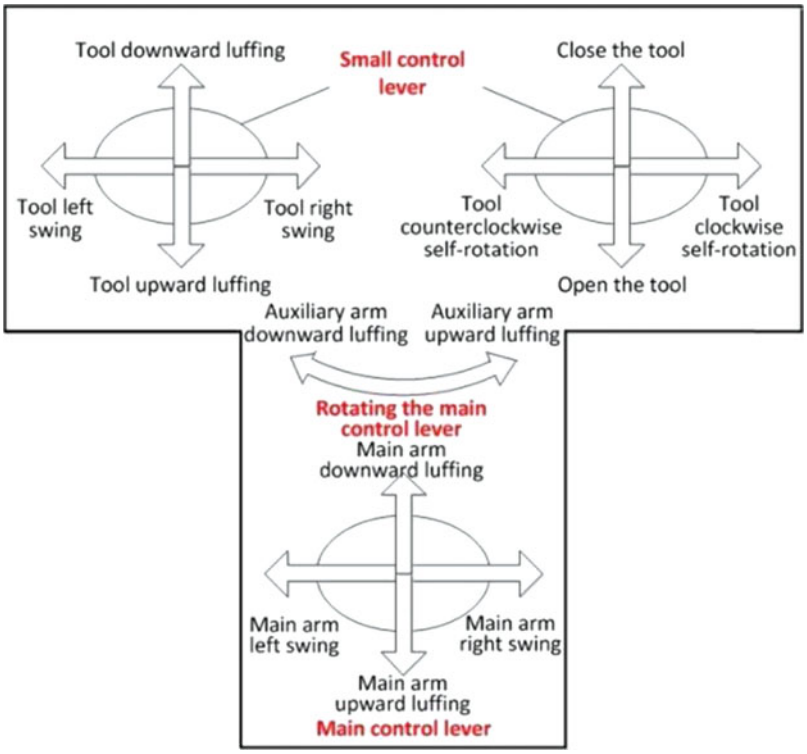


Fig. 6. The meaning of actions of the operating lever in the joint operational mode.

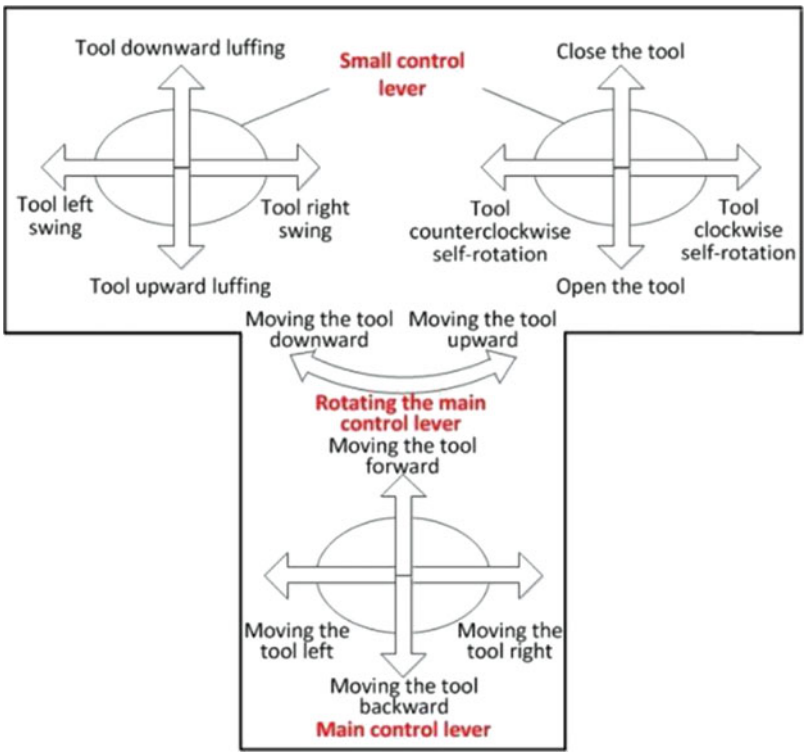


Fig. 7. The meaning of actions of the operating lever in the tool position operational mode.

https://doi.org/10.1017/S0263574714002082 Published online by Cambridge University Press

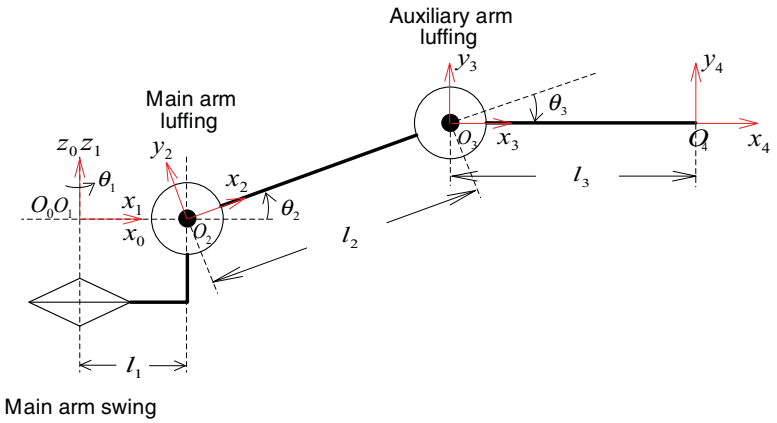


Fig. 8. Model of the single arm of the 20t product.

arm swing, point O_2 is the articulated point between the main arm and the body, point O_3 is the articulated point between the main arm and the auxiliary arm, and point O_4 is the articulated point between the auxiliary arm and the tool, that is, our control target. We hope to employ a reasonable angular velocity of the main arm swing $\dot{\theta}_1$, velocity of the main arm luffing $\dot{\theta}_2$, and velocity of the auxiliary arm luffing $\dot{\theta}_3$ in order to control the motion of point O_4 in an expected direction and linear velocity. The meaning of the three corresponding joint angles is expressed in Fig. 8, where the positive rotational direction of θ_1 is vertical up and $\theta_1 = 0^\circ$ when the plane of the arm is in front of the cab; the positive rotational direction of θ_2 is perpendicular out of the page and $\theta_2 = 0^\circ$ when the main arm is horizontal; the positive rotational direction of θ_3 is perpendicular out of the page and $\theta_2 = 0^\circ$ when the main arm and the auxiliary arm are aligned. The operator uses the operating lever to input the motion information of point O_4, including motion direction and velocity, and the built-in algorithm will solve for the angular velocities $\dot{\theta}_1$, $\dot{\theta}_2$, and $\dot{\theta}_3$ in real time to meet the demand.

According to the knowledge of robotics, there is a linear mapping relationship between the joint velocity vector and the linear velocity vector of the end-effector. The linear transformation between them is realized by the Jacobian, which is associated with the current configuration of the manipulator, then:

$$\dot{\vec{X}} = J \cdot \dot{\vec{\theta}} \tag{1}$$

Referring to the model established in Fig. 8, we have:

$$\dot{\vec{X}} = (\dot{x}_4,\ \dot{y}_4,\ \dot{z}_4)^T,\ \dot{\vec{\theta}} = \left(\dot{\theta}_1, \dot{\theta}_2, \dot{\theta}_3\right)^T$$

$$J = J\left(\theta_1(t), \theta_2(t), \theta_3(t)\right) = \begin{pmatrix} -s_1(l_1 + l_2c_2 + l_3c_{23}) & c_1(-l_2s_2 - l_3s_{23}) & -l_3c_1s_{23} \\ c_1(l_1 + l_2c_2 + l_3c_{23}) & s_1(-l_2s_2 - l_3s_{23}) & -l_3s_1s_{23} \\ 0 & l_2c_2 + l_3c_{23} & l_3c_{23} \end{pmatrix}$$

where $c_1 = cos\theta_1$, $c_{23} = cos\,(\theta_2 + \theta_3)$, and the rest can be deduced by analogy. The meaning of l_1, l_2, and l_3 is indicated in Fig. 8.

We can derive the inverse kinematics algorithm for joint angular velocity vector from Eq. (1):

$$\dot{\vec{\theta}} = J^{-1}(\theta_1, \theta_2, \theta_3) \cdot \dot{\vec{X}} \tag{2}$$

In this way, $J^{-1}(\theta_1, \theta_2, \theta_3)$ in Eq. (2) can be calculated by current joint angle values provided by joint angle sensors in every control cycle, and $\dot{\vec{X}}$, the motion information of the tool, is given by the operating lever. Then, the motion velocities of movement elements, $\dot{\vec{\theta}}$, can be obtained by Eq. (2) in real time. The diagram on the input and the output of the algorithm is shown in Fig. 9.

The obtained joint angular velocities may be supersaturated; that is, the angular velocity is larger than the maximum velocity that the mechanism can actually provide. In this case, we must scale

https://doi.org/10.1017/S0263574714002082 Published online by Cambridge University Press

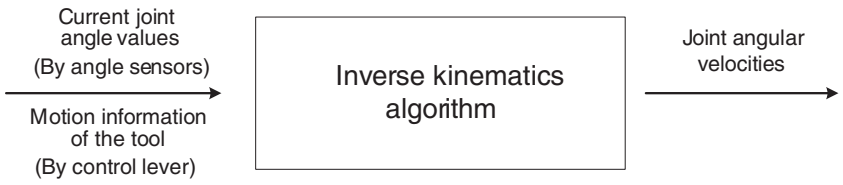


Fig. 9. Diagram of the input and the output of inverse kinematics algorithm.

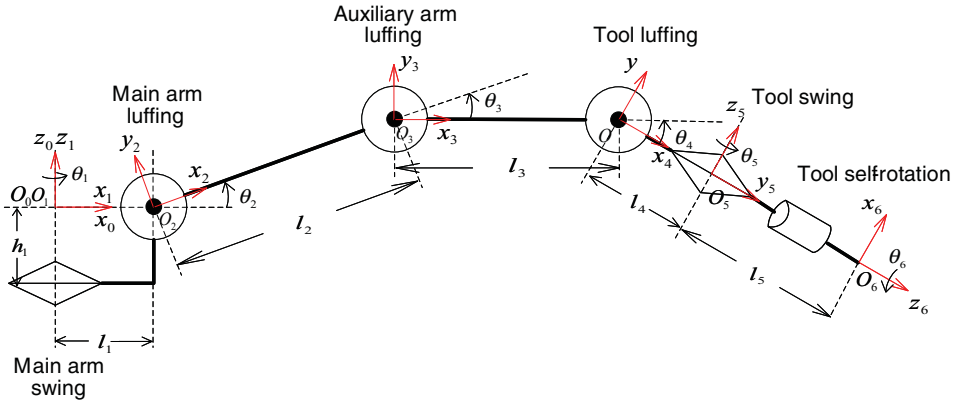


Fig. 10. The diagram of the self-collision avoidance surveillance algorithm.

the theoretical vector of joint angular velocity $\dot{\vec{\theta}}$ down. Because of the limited space, the specific algorithm on scaling is not presented here.

5.3. Self-collision avoidance surveillance issue of the dual arms

Because the dual-arm rescue construction machine with many DOFs is prone to collision between the dual arms in operation, self-collision avoidance is an essential problem. We propose a self-collision avoidance surveillance method to solve this problem. The built-in algorithm of this method can calculate and display the minimum distance between the dual arms in real time. When the minimum distance is larger than the safe distance threshold set in advance, the machine maintains a current running status. And when the minimum distance is smaller than that, the method will give an alarm, make the operating levers invalid, and brake the dual arms. In this way, we can realize the function of monitoring the running status of the dual arms in order to avoid self-collision. At the same time, the operator can avert the potential dangers by observing the trend of changes in the minimum distance in real time. The diagram of the core algorithm is shown in Fig. 10.

In Fig. 10, it is easy to know that a single arm consists of four parts: the main arm (O_2O_3), the auxiliary arm (O_3O_4), the wrist (O_4O_5), and the tool (O_5O_6). In this paper, if one part from the left arm and another part from the right one form one pair of parts, we propose that the distance of any pair of parts needs to be detected and the shortest distance of a total of 16 pairs of parts can be regarded as the minimum distance between the dual arms. In addition, the algorithm can find the pair of parts where the minimum distance occurs. It is worth noting that each part is described with a theoretical link in Fig. 10 without regard to its actual shape.

In Fig. 11, the coordinates of the endpoints of the theoretical links can be calculated by the forward kinematics algorithm of the arm based on the joint angle values detected by angle sensors (refer to appendix A for the specific algorithm). The shortest distance between any pair of theoretical links, that is, the length of the red dashed line in Fig. 11, can be solved for by the specified algorithm mentioned below. Taking the geometrical appearance of actual links into account, we use a SSV to surround each real link.[31] The radius of the sphere is determined by the specific structure parameter of the link, which is regarded as the safe distance threshold for each real link here. Thanks to the characteristics of the SSV, the calculation of the minimum distance between SSVs can be transformed into the calculation of the minimum distance between their inner primitives. That is, the shortest distance

https://doi.org/10.1017/S0263574714002082 Published online by Cambridge University Press

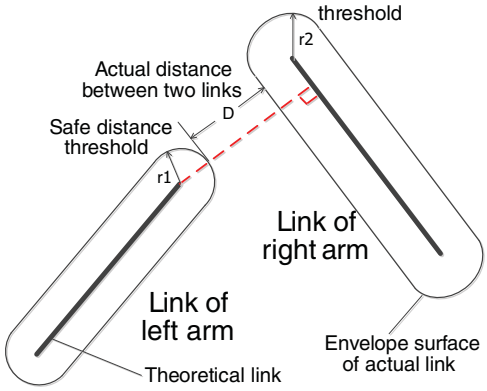


Fig. 11. Diagram of the distance of a pair of actual links.

between two theoretical links minus two safe distance thresholds of the two links can be referred to as the actual shortest distance between the two real links like D shown in Fig. 11.

Based on the discussion above, we can see that the key point of the self-collision avoidance surveillance algorithm is to calculate the shortest distance of a pair of theoretical links. The outline of the corresponding algorithm is presented in the following part. Before the algorithm, two related propositions need to be listed first (the detailed proofs of the propositions are given in appendix B).

Proposition 1: the shortest distance between two segments in the same plane that do not intersect must occur at one end point of one of the two segments.

Proposition 2: there are two arbitrary segments, AB and CD, in different planes. Plane α is perpendicular to the common perpendicular of the two segments and pass through segment AB, and plane β is perpendicular to the common perpendicular and pass through segment CD. C'D' is the projection of CD onto the plane α. The shortest distance between segments, AB and CD, is the square root of the sum of the square of the shortest distance between segments, AB and C'D', and the square of the distance between planes α and β.

The outline of the algorithm of the shortest distance Dm between two spatial arbitrary segments, AB and CD (correspond to a pair of theoretical links) is as follows (see also appendix C for the detailed algorithms):

If segment AB and segment CD are aligned

If AB and CD are overlapped

Then Dm = 0

Else AB and CD are not overlapped

Then Dm = min(AC, AD, BC, BD)

(The right part of the equation denotes selecting the minimum length of segments, AC, AD, BC, and BD.)

Else if AB and CD are in the same plane

If AB and CD are intersectant

Then Dm = 0

Else AB and CD are not intersectant

Then Dm = min(min(A,CD), min(B,CD), min(C,AB), min(D,AB))

(Formula (min(A,CD) indicates the shortest distance between point A and segment CD.)

Else AB and CD are in different planes

If AB and C'D' are intersectant

Then Dm = the distance between α and β

Else AB and C'D' are not intersectant

Then Dm =

$$\sqrt{\begin{array}{c}\text{the shortest distance between AB and } C'D'^2 + \\ \text{the distance between } \alpha \text{ and } \beta^2\end{array}}$$

https://doi.org/10.1017/S0263574714002082 Published online by Cambridge University Press

Table VII. Manipulation and movement sequences of grip-and-cut task.

Subtask of gripping object (left arm: grab)			Subtask of cutting object (right arm: hydraulic shear)		
1	Preparation manipulation	Move the grab to approach the target (movement primitive) Adjust the orientation of the grab by tool luffing, swing, and self-rotation (movement element)	1	Suspension manipulation	
2	Executing manipulation	Close the grab (movement element)			
3	Raising manipulation	Move the grab upward (movement primitive) Adjust the posture of the grab (movement element)			
4	Suspension manipulation		2	Preparation manipulation	Move the hydraulic shear to approach target (movement primitive) Adjust the orientation of the hydraulic shear by tool luffing, swing, and selfrotation (movement element)
			3	Executing manipulation	Movement of hydraulic shear (movement element)

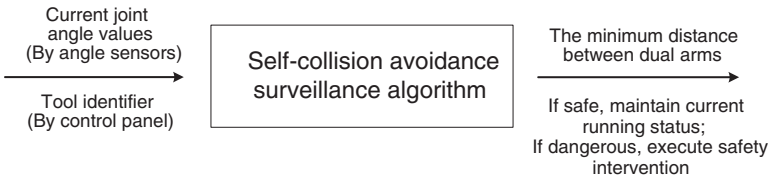


Fig. 12. Diagram of the input and the output of the self-collision avoidance surveillance algorithm.

Based on the joint angle values provided by sensors and current tool identifiers inputted by the operator through the control panel (related to the safe distance threshold of the tool), the algorithm can calculate the minimum distance of a total of 16 pairs of links between the dual arms and indicate the pair of links where the minimum distance happens in real-time. This information can be provided for the operator to monitor the running status of the machine. The diagram on the input and the output of the algorithm is shown in Fig. 12.

6. A Simulation Example of the 20t Intelligent Dual-Arm Rescue Construction Machine

In this section, a simulation of the classic grip-and-cut task is performed for the 20t intelligent dual-arm rescue construction machine. According to the library shown in Fig. 4, the manipulation and movement sequences of this task can be designed and described in Table VII.

Assuming the initial configurations of dual arms are both $\theta_1 = 0^\circ, \theta_2 = 60^\circ, \theta_3 = -90^\circ, \theta_4 = 0^\circ, \theta_5 = 0^\circ$ as shown in Fig. 13:

https://doi.org/10.1017/S0263574714002082 Published online by Cambridge University Press

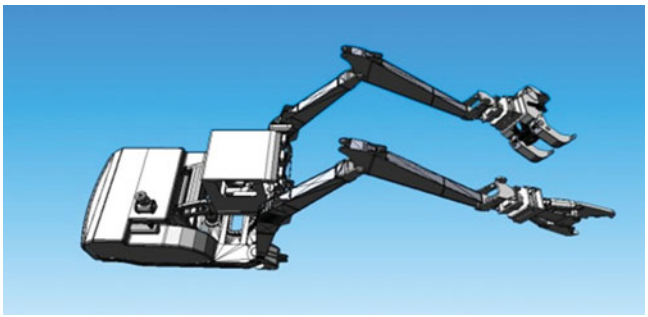


Fig. 13. Initial configurations of dual arms for the 20t intelligent dual-arm rescue construction machine.

The task-motion planning of the grip-and-cut task is made according to Table VII. First, the movement primitive of moving the tool, that is, the tool position operational mode is employed to make the articulated point between the auxiliary arm and the wrist of left arm move from the initial position (4890,0,2636)(mm) to target position (5790,0,2936)(mm) with a velocity vector (300,0,100)(mm/s) for 3 s in order to adjust the position of grab (all the data are described relative to frame 0 in Fig. 8 or Fig. 10, the same below). Second, the orientation of the tool is adjusted toward vertical down by the movement element of tool luffing in joint operational mode in order to grab the target object, and its running time is 1 s. Third, the movement primitive of moving the tool is used again to make the articulated point move to (5790,0,3936)(mm) with a velocity vector (0,0,200) (mm/s) for 5 s, and then the orientation of the tool is readjusted toward vertical down for 1 s. Next, the left arm keeps static, and the articulated point between the auxiliary arm and the wrist of right arm moves to position (5790,300,1936)(mm) with a velocity vector (180,60,140)(mm/s) for 5 s by means of the same movement primitive. Finally, the orientation of the hydraulic shear is adjusted by two movement elements of tool luffing and tool swing for 1 s respectively in order to cut the object grabbed by the left arm. The specific process is shown in Fig. 14, and the total time is 17 s. Each joint trajectory in the whole process of the grip-and-cut task is shown in Fig. 15. And the profile of the shortest distance between the dual arms for this task is obtained by using the self-collision avoidance surveillance algorithm and is presented in Fig. 16, where the profile is basically in correspondence with the situations shown in Fig. 14. According to the result in the figure, it is known that the operator will not be alarmed during this task and the operation of the dual arms will be carried out successfully if the safe distance threshold is set to be 100 mm in advance.

For comparison, the traditional operation method of construction machinery, the pure joint operational mode, is employed to operate the dual arms to achieve the same grip-and-cut task again from the same initial configurations. In this mode, the operator can only operate a single joint at each operational action with the operating lever, so that the operator has to operate different joints many times in turn to perform complicated tasks. In this case, in order to compare the traditional operation method with the proposed operation method, the six key configurations of the dual arms shown in Fig. 14 are also required to be attained in the joint operational mode, that is:

Key configurations 1:
Left arm: (0°, 50.88°, −64.87°, 0°, 0°)
Right arm: (0°, 60°, −90°, 0°, 0°)
Key configurations 2:
Left arm: (0°, 50.88°, −64.87°, −76.01°, 0°)
Right arm: (0°, 60°, −90°, 0°, 0°)
Key configurations 3:
Left arm: (0°,51.97°, −46.4°, −76.01°, 0°)
Right arm: (0°, 60°, −90°, 0°, 0°)
Key configurations 4:
Left arm: (0°, 51.97°, −46.4°, −95.58°, 0°)
Right arm: (0°, 60°, − 90°, 0°, 0°)
Key configurations 5:

https://doi.org/10.1017/S0263574714002082 Published online by Cambridge University Press

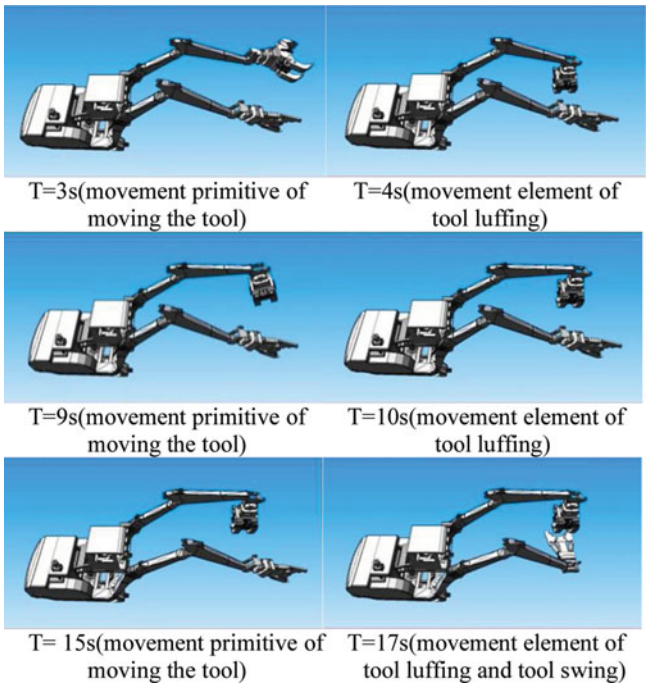


Fig. 14. Simulation of classic grip-and-cut task for the 20t intelligent dual-arm rescue construction machine.

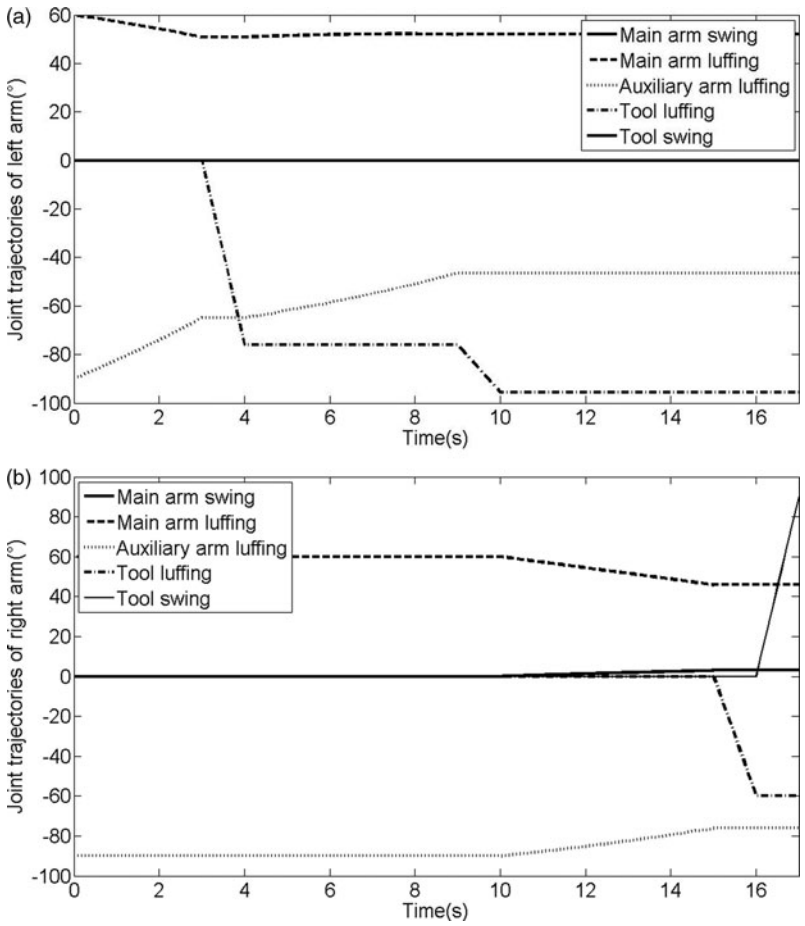


Fig. 15. Joint trajectories of the grip-and-cut task for the dual arms in the proposed operational mode.

https://doi.org/10.1017/S0263574714002082 Published online by Cambridge University Press

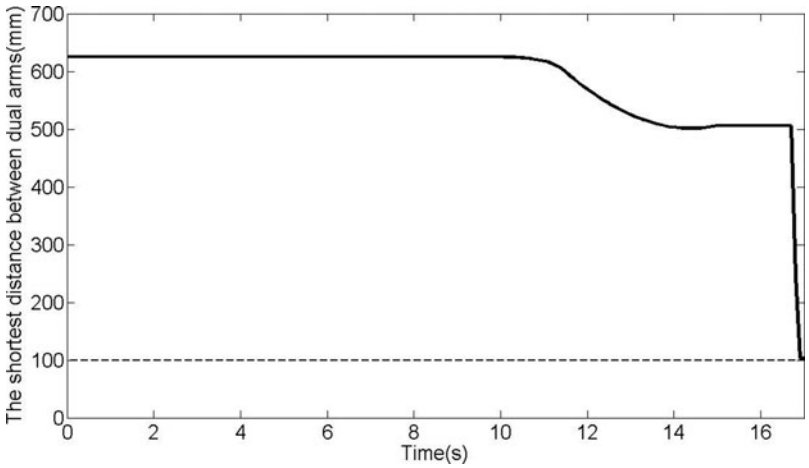


Fig. 16. The profile of the shortest distance between the dual arms during the grip-and-cut task.

Left arm: (0°, 51.97°, −46.4°, −95.58°, 0°)
Right arm: (2.97°, 45.87°, − 76.10°, 0°, 0°)
Key configurations 6:
Left arm: (0°, 51.97°, −46.4°, −95.58°, 0°)
Right arm: (2.97°, 45.87°, −76.10°, −59.76°, 90°)

When using the traditional operation method to control the dual arms to carry out the same task, the angular velocity of each joint is set to its maximum angular velocity employed in the proposed operation method, which can be obtained by the previous simulation results:

$$\dot{\theta}_{1\max_left} = 0(^\circ/s), \quad \dot{\theta}_{1\max_right} = 0.70(^\circ/s),$$
$$\dot{\theta}_{2\max_left} = 3.58(^\circ/s), \quad \dot{\theta}_{2\max_right} = 2.89(^\circ/s),$$
$$\dot{\theta}_{3\max_left} = 9.57(^\circ/s), \quad \dot{\theta}_{3\max_right} = 3.44(^\circ/s),$$
$$\dot{\theta}_{4\max_left} = 76.01(^\circ/s), \quad \dot{\theta}_{4\max_right} = 59.76(^\circ/s),$$
$$\dot{\theta}_{5\max_left} = 0(^\circ/s), \quad \dot{\theta}_{5\max_right} = 90(^\circ/s).$$

The simulation results of joint trajectories for the same grip-and-cut task performed in the joint operational mode are shown in Fig. 17.

Comparing Fig. 17 with Fig. 15, it is easy to find that the total time of the grip-and-cut task by using the traditional operation method, 23.84 s, is larger than the total time when using the proposed operation method, 17 s, even though the angular velocity of each joint used in the traditional operation method is set to be its maximum velocity employed in the proposed operation method. In addition, the number of operational actions is 6 in the proposed operation method, whereas the number is increased up to 11 in the traditional operation method. So, if taking the intervals between operational actions in the actual operation situation into account, the operational time it takes in the traditional method will even be much longer than the operational time it takes in the proposed method. On the other hand, in the traditional operation method, the lever operational actions have little intuitive relationship with the corresponding arm movements; the operator cannot operate the rescue construction machine with many DOFs intuitively, which will increase the mental effort of the operator and reduce the operational efficiency. In other research, to solve this problem, a novel operation device is developed and installed on ASTACO produced by Hitachi Construction Machinery[32] (not used in this case). The operational device includes two specialized levers that control the two arms separately. By arranging all the lever actions in the operational device elaborately, the direction of each lever movement is almost equivalent to the direction of its corresponding arm movement. Therefore, the operator can operate the dual arms on ASTACO intuitively by using the two specialized levers. However, because the operational device still has many lever movements like the traditional lever,

https://doi.org/10.1017/S0263574714002082 Published online by Cambridge University Press

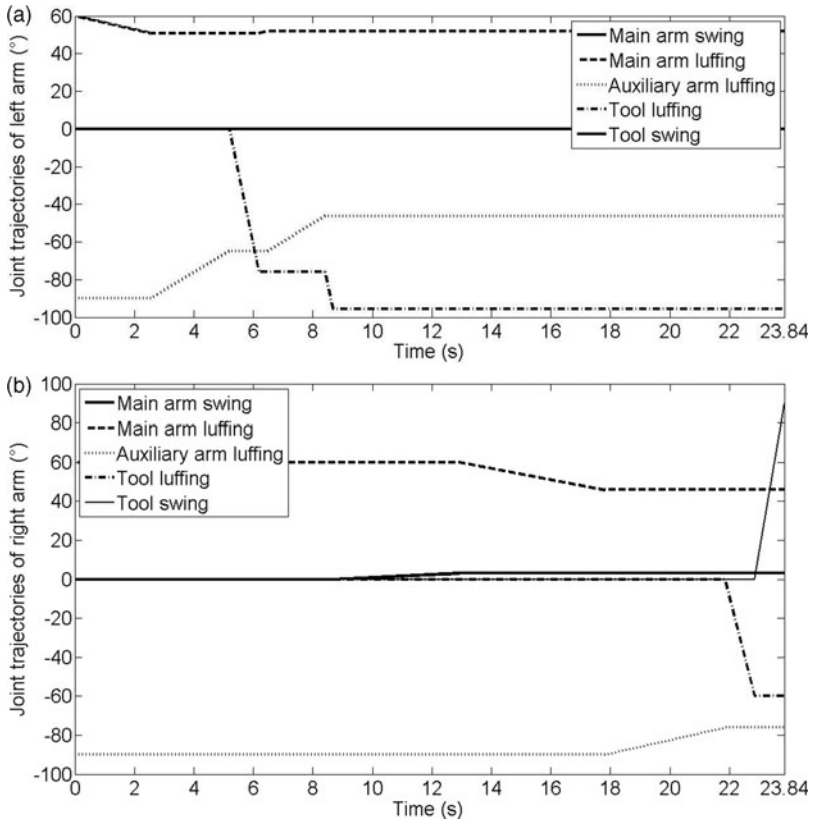


Fig. 17. Joint trajectories of the grip-and-cut task for the dual arms in the traditional joint operational mode.

Mitsuhiro Kamezaki[33] developed an operator support system to provide the auxiliary informational and operational support during different operational phases in order to help the operator achieve the complicated tasks better. From the perspective of intuitiveness, the intuitively movement-based operation method can be also regarded as an auxiliary operational support to reduce the mental effort of the operator when operating the machines with many degrees of freedom. In addition, because of the coordinated motions of multiple joints at one operational action, the movement-based operation method can effectively reduce the total operation time to increase the operational efficiency of the operator, which is very important for the rescue application.

7. Conclusion

A novel operation method for dual-arm rescue construction machinery is inspired by the operating strategies of the human dual arms, that is, complicated tasks can be decomposed into several large manipulation phases and some meaningful movement primitives in order. For any specialized dual-arm rescue construction machine, according to the decomposition results of the main tasks faced by rescue construction machinery in terms of relatively independent manipulations and movements, some frequently used movements can be found to design movement primitives that will move several basic movement elements simultaneously to realize an intuitive motion effect. Movement primitives with multi-joint coordinated motion and movement elements with single-joint motion constitute a movement library for rescue construction machinery, which forms a novel hybrid operation method. The use of movement library can not only improve the operational efficiency of the operator but also alleviate his operational burden. The technical details of the method are presented by means of a case example of a 20t intelligent dual-arm rescue construction machine product. The feasibility and effectiveness of the proposed operation method are validated by a simulation of a typical grip-and-cut task.

https://doi.org/10.1017/S0263574714002082 Published online by Cambridge University Press

Acknowledgments
The support for this research by National Key Technology R&D Program (No. 2011BAF04B01) and NSFC National Science Fund for Distinguished Young Scholars (No. 51125020) is greatly appreciated. And the authors would like to also thank engineer Zheng Xu from China Academy of Machinery Science & Technology for his help with simulation environment support.

References

1. DLR, Mobile Humanoid "Justin", http://www.dlr.de/rm/en/desktopdefault.aspx/tabid-4789/7945_read-12712/,2008.
2. NASA, Robonaut2, http://robonaut.jsc.nasa.gov/default.asp, 2012.
3. Hitachi Construction Machinery, ASTACO NEO, http://www.hitachi-kenki.co.jp/products/hot/astaco_neo/index.html, 2011.
4. Tmsuk, T53, http://www.tmsuk.co.jp/topic/robot/ t53enryu/,2007.
5. C. Smith *et al.*, "Dual arm manipulation—a survey," *Robot. Auton. Syst.* **60**(10), 1340–1353 (2012).
6. Y. Yamada, S. Nagamatsu and Y. Sato, "Development of Multi-Arm Robots for Automobile Assembly," *IEEE International Conference on Robotics and Automation*, Nagoya, Japan, (1995) pp. 2224–2229.
7. Y. F. Zheng and M. Z. Chen, "Trajectory planning for two manipulators to deform flexible beams," *Robot. Auton. Syst.* **12**(1–2), 55–67 (1994).
8. J. Maitin-Shepard, M. Cusumano-Towner, J. Lei and P. Abbeel, "Cloth Grasp Point Detection based on Multiple-View Geometric Cues with Application to Robotic Towel Folding," *IEEE International Conference on Robotics and Automation*, Anchorage, Alaska, (2010) pp. 2308–2315.
9. T. Mukai, S. Hirano, H. Nakashima, Y. Kato, Y. Sakaida, S. Guo and S. Hosoe, "Development of a Nursing-Care Assistant Robot Riba that can Lift a Human in its Arms," *IEEE/RSJ International Conference on Intelligent Robots and Systems*, Taipei, Taiwan, (2010) pp. 5996–6001.
10. T. Wimböck and C. Ott, "Dual-Arm Manipulation," *Towards Service Robots for Everyday Environments, Springer Tracts in Advanced Robotics*, vol. 76, (Springer, Berlin Heidelberg, 2012) pp. 353–366.
11. A. Edsinger and C. C. Kemp, "Two Arms are Better Than One: A Behavior-Based Control System for Assistive Bimanual Manipulation," *Recent Progress in Robotics: Viable Robotic Service to Human. Lecture Notes in Control and Information Sciences*, vol. 370, (Springer, Berlin Heidelberg, 2008) pp. 345– 355.
12. S. Schaal, S. Kotosaka and D. Sternad, "Nonlinear Dynamical Systems as Movement Primitives," *IEEE International Conference on Humanoid Robotics*, Cambridge, USA (2000) pp. 1–11.
13. S. Tadokoro, T. Takamori, K. Osuka and S. Tsurutani, "Investigation Report of the Rescue Problem at Hanshin-Awaji Earthquake in Kobe," *IEEE/RSJ International Conference on Intelligent Robots and Systems,* Takamatsu, Japan (2000) pp. 1880–1885.
14. T. Asfour, P. Azad, F. Gyarfas and R. Dillmann, "Imitation learning of dual-arm manipulation tasks in humanoid robots," *Int. J. Humanoid Robot.* **5**(2), 289–308 (2008).
15. R. V. Patel, F. Shadpey, F. Ranjbaran and J. Angeles, "A collision-avoidance scheme for redundant manipulators theory and experiments," *J. Robot. Syst.* **22**(12), 737–757 (2005).
16. R. G. Chittawadigi and S. K. Saha, "An Analytical Method to Detect Collision between Cylinders Using Dual Number Algebra," *International Conference onIntelligent Robots and Systems,* Tokyo, Japan, (2013) pp. 5353–5358.
17. K. Okada, M. Inaba and H. Inoue, "Real-Time and Precise Self Collision Detection System for Humanoid Robots," *International Conference on Robotics and Automation,* Barcelona, Spain, (2005) pp. 1072–1077.
18. T. C. Hudson, M. C. Lin, J. Cohen, S. Gottschalk and D. Manocha, "V-COLLIDE: Accelerated Collision Detection for VRML," *Proceedings of 2nd Annual Symposium on the Virtual Reality Modelling Language*, Monterey, USA, (1997) pp. 117–124.
19. K. Okada and M. Inaba, "A Hybrid Approach to Practical Self Collision Detection System of Humanoid Robot," *International Conference on Intelligent Robots and Systems*, Beijing, China, (2006) pp. 3952–3957.
20. T. Flash and B. Hochner, "Motor primitives in vertebrates and invertebrates," *Curr. Opin. Neurobiol.* **15**(6), 660–666 (2005).
21. F. A. Mussa-Ivaldi and S. A. Solla, "Neural primitives for motion control," *IEEE J. Ocean. Eng.* **2**(3), 640–650 (2004).
22. F. A. Mussa-Ivaldi and E. Bizzi, "Motor learning through the combination of primitives," *Philos. Trans. R. Soc. Lon. B, Biol. Sci.* **355**, 1755–1769 (2000).
23. F. A. Mussa-Ivaldi and S. A. Solla, "Neural primitives for motion control," *IEEE J. Ocean. Eng.* **2**(3), 640–650 (2004).
24. D. Hestenes, "Invariant body kinematics: II. Reaching and neurogeometry," *Neural Netw.* **7**(1), 79–81 (1994).
25. J. Kober and J. Peters, "Imitation and reinforcement learning practical algorithms for motor primitives in robotics," *IEEE Robot. Autom. Mag.* **17**(2), 55–62 (2010).
26. S. M. Pellis, "Conservative motor systems, behavioral modulation and neural plasticity," *Behav. Brain Res.* **214**(1), 25–29 (2010).
27. S. F. Giszter and C. B. Hart, "Biomimetic control for redundant and high degree of freedom limb systems: neurobiological modularity," *Smart Struct. Syst.* **7**(3), 169–184 (2011).

https://doi.org/10.1017/S0263574714002082 Published online by Cambridge University Press

28. K. Pastra and Y. Aloimonos, "The minimalist grammar of action," *Phil. Trans. R. Soc. B-Biol. Sci.* **367**(1585), 103–117 (2012).
29. X. Ding and C. Fang, "A novel method of motion planning for an anthropomorphic arm based on movement primitives," *IEEE/ASME Trans. Mechatronics* **18**(2), 624–636 (2013).
30. J. Denavit and R. S. Hartenberg, "A kinematic notation for lower-pair mechanisms based on matrices," *J. Appl. Mech.* **22**(1), 215–221 (1955).
31. C. Ericson, *Real-Time Collision Detection* (Morgan Kaufmann, San Francisco, 2005).
32. A. Ishii, "Operation System of a Double-Front Work Machine for Simultaneous Operation," *23rd International Symposium Automation and Robotics in Construction*, Tokyo, Japan, (2006) pp. 539–542.
33. M. Kamezaki, H. Iwata and S. Sugano, "Operator support system based on primitive static states in intelligent operated work machines," *Adv. Robot.* **23**(10), 1281–1297 (2009).

Appendix A:

Solve for the coordinates of the end points of each theoretical link by forward kinematics algorithm.

In every control cycle, firstly given $\theta_{l1}, \theta_{l2}, \theta_{l3}, \theta_{l4}, \theta_{l5}, \theta_{r1}, \theta_{r2}, \theta_{r3}, \theta_{r4}, \theta_{r5}$ (shown in Fig. 10) provided by angle sensors, where θ_{l1} denotes the theoretical rotational angle of the main arm swing for the left arm and θ_{r1} expresses that for the right arm. Subscripts, l and r, are used to indicate the left arm and the right arm. Then, we can calculate the coordinates of the end points of the theoretical links for dual arms: $O_{l2}, O_{l3}, O_{l4}, O_{l5}, O_{l6}, O_{r2}, O_{r3}, O_{r4}, O_{r5}, O_{r6}$. The mathematical expressions for them are as follows:

$$O_{l2} = \begin{pmatrix} l_1 c_{l1} \\ l_1 s_{l1} + l_0 \\ 0 \end{pmatrix}, \quad O_{l3} = \begin{pmatrix} c_{l1}(l_1 + l_2 c_{l2}) \\ s_{l1}(l_1 + l_2 c_{l2}) + l_0 \\ l_2 s_{l2} \end{pmatrix}$$

$$O_{l4} = \begin{pmatrix} c_{l1}(l_1 + l_2 c_{l2} + l_3 c_{l23}) \\ s_{l1}(l_1 + l_2 c_{l2} + l_3 c_{l23}) + l_0 \\ l_2 s_{l2} + l_3 s_{l23} \end{pmatrix}$$

$$O_{l5} = \begin{pmatrix} c_{l1}(l_1 + l_2 c_{l2} + l_3 c_{l23} + l_4 c_{l234}) \\ s_{l1}(l_1 + l_2 c_{l2} + l_3 c_{l23} + l_4 c_{l234}) + l_0 \\ l_2 s_{l2} + l_3 s_{l23} + l_4 s_{l234} \end{pmatrix}$$

$$O_{l6} = \begin{pmatrix} c_{l1}(l_1 + l_2 c_{l2} + l_3 c_{l23} + l_4 c_{l234}) + l_{l5}(c_{l1} c_{l234} c_{l5} - s_{l1} s_{l5}) \\ s_{l1}(l_1 + l_2 c_{l2} + l_3 c_{l23} + l_4 c_{l234}) + l_{l5}(s_{l1} c_{l234} c_{l5} + c_{l1} s_{l5}) + l_0 \\ l_2 s_{l2} + l_3 s_{l23} + l_4 s_{l234} + l_{l5} s_{l234} c_{l5} \end{pmatrix}$$

$$O_{r2} = \begin{pmatrix} l_1 c_{r1} \\ l_1 s_{r1} \\ 0 \end{pmatrix}, \quad O_{r3} = \begin{pmatrix} c_{r1}(l_1 + l_2 c_{r2}) \\ s_{r1}(l_1 + l_2 c_{r2}) \\ l_2 s_{r2} \end{pmatrix}$$

$$O_{r4} = \begin{pmatrix} c_{r1}(l_1 + l_2 c_{r2} + l_3 c_{r23}) \\ s_{r1}(l_1 + l_2 c_{r2} + l_3 c_{r23}) \\ l_2 s_{r2} + l_3 s_{r23} \end{pmatrix}$$

$$O_{r5} = \begin{pmatrix} c_{r1}(l_1 + l_2 c_{r2} + l_3 c_{r23} + l_4 c_{r234}) \\ s_{r1}(l_1 + l_2 c_{r2} + l_3 c_{r23} + l_4 c_{r234}) \\ l_2 s_{r2} + l_3 s_{r23} + l_4 s_{r234} \end{pmatrix}$$

$$O_{r6} = \begin{pmatrix} c_{r1}(l_1 + l_2 c_{r2} + l_3 c_{r23} + l_4 c_{r234}) + l_{r5}(c_{r1} c_{r234} c_{r5} - s_{r1} s_{r5}) \\ s_{r1}(l_1 + l_2 c_{r2} + l_3 c_{r23} + l_4 c_{r234}) + l_{r5}(s_{r1} c_{r234} c_{r5} + c_{r1} s_{r5}) \\ l_2 s_{r2} + l_3 s_{r23} + l_4 s_{r234} + l_{r5} s_{r234} c_{r5} \end{pmatrix}$$

https://doi.org/10.1017/S0263574714002082 Published online by Cambridge University Press

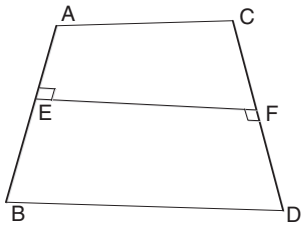


Fig. 18. The shortest distance between two segments in the same plane.

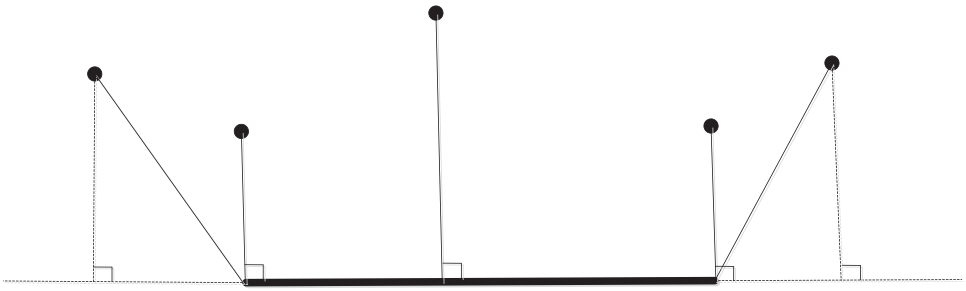


Fig. 19. Five situations of the shortest distance between a point and a segment.

l_0 is the distance between two articulated points that are between the machine body and each arm. Because the origin of the base frame is set at point O_{l0} of the right arm, every y-axis coordinate of the endpoint of the theoretical link of the left arm described in the base frame equals the y-axis coordinate described in frame 0 of the left arm plus l_0. In addition, the values of l_{l5} and l_{r5} vary as the tools of dual arms change.

Appendix B:

Proof of proposition 1:

In Fig. 18, assuming that the shortest distance between segments AB and CD does not occur at the end point of the segment, that is, the two endpoints of the segment of the shortest distance, E and F, are located in the middle of segments AB and CD, respectively, then the length of EF is the shortest distance between point E and segment CD. It is well-known that the shortest distance between a point and a line is the length of the perpendicular between them. And for a segment, there are five situations shown in Fig. 19: the foot of the perpendicular is in the middle of the segment, or is at its two end points, or is in the two extension lines at its both sides. It is not difficult to summarize that from Fig. 19: if the shortest distance between a point and a segment occurs in the middle of the segment, the segment of the shortest distance must be the perpendicular segment. Hence, EF is perpendicular to CD because the length of EF is the shortest distance between E and CD, and F is in the middle of CD. And vice versa, F is perpendicular to AB. So, it can be deduced that AB is parallel to CD. That is to say, two segments are parallel when the shortest distance does not occur at the endpoint of the segment, so the segment of the shortest distance can be substituted with AC or BD shown in Fig. 17. So the proposition is proven.

Proof of proposition 2:

As shown in Fig. 20, the distance between an arbitrary point E in line AB and an arbitrary point F in line CD can be expressed: $\mathrm{EF} = \sqrt{\mathrm{EF}'^2 + \mathrm{FF}'^2}$. Where FF′ denotes the distance between two planes, α and β, which is a constant. So, the length of EF is a monotonic increasing function of the length of EF′, that is, if the length of EF′ is the shortest distance between AB and C′D′ in the same plane, the length of EF is the shortest distance between AB and CD in different planes. Thus, the problem on the shortest distance between two segments, AB and CD, in different planes degenerates into the issue on the shortest distance between AB and C′D′, the projection of CD, in the same plane. So, the shortest length of EF can be calculated by the formula mentioned above after finding the shortest length of EF′. The proposition is proven.

https://doi.org/10.1017/S0263574714002082 Published online by Cambridge University Press

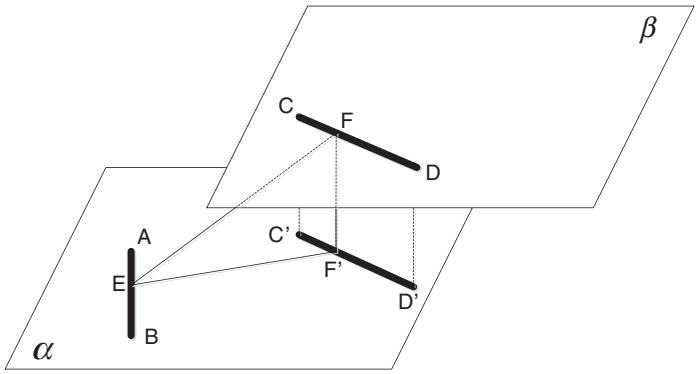


Fig. 20. The shortest distance between two segments in the different planes.

Appendix C:
Assume P_A, P_B, P_C, P_D represent the position vectors of points A, B, C, D, respectively.

Algorithm of identifying different situations:

$P_{AC} = P_C - P_A, \quad P_{BC} = P_C - P_B,$

$P_{AD} = P_D - P_A, \quad P_{BD} = P_D - P_B,$

If $P_{AC} \times P_{BC} = 0$ and $P_{AD} \times P_{BD} = 0$

Then segment AB and segment CD are aligned.

Elseif $P_{AC} \times P_{BC} = 0$ or $P_{AD} \times P_{BD} = 0$

Then segment AB and segment CD are in the same plane.

Else

If $(P_{AC} \times P_{BC}) \times (P_{AD} \times P_{BD}) = 0$

Then segment AB and segment CD are in the same plane.

Else

Then segment AB and segment CD are in different planes.

The symbol $\times$ denotes the cross product between vectors.

Algorithm of calculating the shortest distance between segments AB and CD when they are aligned (one-dimensional situation):

$P_{AB} = P_B - P_A, \quad P_{CD} = P_D - P_C$

$l_{\max} = \max\left(\|P_{AC}\|, \|P_{BC}\|, \|P_{AD}\|, \|P_{BD}\|\right)$

If $l_{\max} \leq \|P_{AB}\| + \|P_{CD}\|$

https://doi.org/10.1017/S0263574714002082 Published online by Cambridge University Press

Then $D_m = 0$

Else

Then $D_m = \min\left(\|P_{AC}\|, \|P_{BC}\|, \|P_{AD}\|, \|P_{BD}\|\right)$

Where symbol $\|\cdot\|$ indicates the magnitude of vector.

Algorithm of calculating the shortest distance between segments AB and CD when they are in the same plane (two-dimensional situation):

$\angle BCA = acos\left(\frac{\|P_{AC}\|^2+\|P_{BC}\|^2-\|P_{AB}\|^2}{2\|P_{AC}\|\|P_{BC}\|}\right)$

$\angle CAB = acos\left(\frac{\|P_{AC}\|^2+\|P_{AB}\|^2-\|P_{BC}\|^2}{2\|P_{AC}\|\|P_{AB}\|}\right)$

$P_{CA} = -P_{AC}, \quad P_{CB} = -P_{BC}$

If $\frac{P_{CB}\times P_{CA}}{\|P_{CB}\times P_{CA}\|} = \frac{P_{CD}\times P_{CA}}{\|P_{CD}\times P_{CA}\|}$

Then $\angle DCA = acos(\frac{P_{CA}}{\|P_{CA}\|}\cdot\frac{P_{CD}}{\|P_{CD}\|})$

Else

Then $\angle DCA = -acos(\frac{P_{CA}}{\|P_{CA}\|}\cdot\frac{P_{CD}}{\|P_{CD}\|})$

End

If $0 \le \angle DCA \le \angle BCA$

If $\|P_{CD}\| \ge \|P_{AC}\|\frac{\sin(\angle CAB)}{\sin(\pi-\angle CAB-\angle DCA)}$

Then $D_m = 0$

Else

Then $D_m = \min(\min(A, CD), \min(B, CD), \min(C, AB), \min(D, AB))$

Else

Then $D_m = \min(\min(A, CD), \min(B, CD), \min(C, AB), \min(D, AB))$

where symbol $\cdot$ denotes the dot product between vectors, and the shortest distance between a point and a segment like $\min(A, CD)$ can be computed by using standard methods.

Algorithm of calculating the shortest distance between segments AB and CD when they are in different planes (three-dimensional situation):

$L = \frac{P_{AB}\times P_{CD}}{\|P_{AB}\|\times\|P_{CD}\|}$

If $P_{CA}\cdot L > 0$

Then $D_1 = P_{CA}\cdot L$

Else

https://doi.org/10.1017/S0263574714002082 Published online by Cambridge University Press

Then $D_1 = -P_{CA} \cdot L$

$L = -L$

End

$P_{C'} = P_C + D_1 L$

$P_{D'} = P_D + D_1 L$

Assume D_2 indicates the shortest distance between segments AB and C′D′, which can be calculated by the algorithm of two-dimensional situation, then:

$$D_m = \sqrt{D_1^2 + D_2^2},$$

where L indicates the unit direction vector of the common perpendicular of segments AB and CD, and D_1 denotes the distance between planes α and β.

https://doi.org/10.1017/S0263574714002082 Published online by Cambridge University Press